Mutagenic Evidence for the Optimal Control of Evolutionary Dynamics

Raj Chakrabarti,* Herschel Rabitz, Stacey L. Springs, and George L. McLendon

Department of Chemistry, Princeton University, Princeton, New Jersey 08544, USA

(Received 4 November 2007; revised manuscript received 6 February 2008; published 24 June 2008)

Elucidating the fitness measures optimized during the evolution of complex biological systems is a major challenge in evolutionary theory. We present experimental evidence and an analytical framework demonstrating how biochemical networks exploit optimal control strategies in their evolutionary dynamics. Optimal control theory explains a striking pattern of extremization in the redox potentials of electron transport proteins, assuming only that their fitness measure is a control objective functional with bounded controls.

DOI: 10.1103/PhysRevLett.100.258103 PACS numbers: 87.23.−n, 02.30.Yy, 87.15.−v

Evolution is guided by the optimization of fitness measures that balance functionally beneficial properties. In modern theories of evolutionary dynamics, such as the quasispecies model [1] and variants thereof, the fitness measure of a biological system plays a role analogous to that of the free energy of a mechanical system. The dynamics of the system, embodied through mutations, seeks to optimize this measure. Recently, with advances in the understanding of molecular biophysics, increasing attention has been paid to characterizing the fitness measures underlying the evolution of proteins. For example, simulations of protein sequence evolution have confirmed that protein cores evolve almost universally to maximize the free energy gap between the folded and denatured states [2]. However, for functional properties of proteins and protein networks, the appropriate biological fitness measures are not so clear [3]. A current challenge in evolutionary theory is to identify how the fitness measures of complex biological systems depend on the physical properties of their constituent proteins.

In the hierarchical evolution of protein networks, biological self-organization [4] influences the dynamics that occur on shorter time scales. Although most theories of evolutionary dynamics have modeled evolution as a dynamical system seeking to optimize a potential or free energy, multi-time-scale evolution of protein networks may be modeled within a broader framework as a control problem. Optimal control (OC) theory is generally concerned with the determination of the time-dependent functional form of the Hamiltonian of a controlled dynamical system that maximizes a desired objective function [5]. An important difference between a dynamical system and a control system is that the latter distinguishes between the free dynamics of the system and the dynamics regulated by controls. In the present case, these controls can take the form of functional protein properties.

The evolution of a biological system may be modeled as a control system if the regulatory functional properties of its constituent proteins coevolve with the network's overall function. Should the evolutionary dynamics of such a system demonstrate features indicative of *optimal* controls, this would constitute evidence that the system's evolution has attained a sophisticated level of self-organization amounting to the solution of an OC problem. Here, we show that application of this theory to active site mutations in an enzyme network of central importance for metabolism—the electron transport chain [6]—indicates that the redox potentials of electron transport proteins are controlling the evolutionary dynamics of this network in an optimal fashion, providing insight into the self-organization of this system.

The mitochondrial electron transport chain (ETC) removes electrons from the high-energy electron donor NADH and passes them to the electron acceptor O_2 through a series of redox reactions involving electron transport proteins. These reactions are coupled to the generation of a proton concentration gradient across the mitochondrial inner membrane, which is ultimately used to produce adenosine triphosphate (ATP). Our prior work [7,8] pursued a strategy of examining "evolution in reverse" with the four-helix bundle ETC hemoprotein cytochrome b_{562}. Starting with the evolved protein, variants with replacements at amino acids near the active site heme were created and examined for redox function. We found two general results. First, within this conserved protein architecture, a range of variation in redox potential ε^0 of about 160 mV could be obtained within two rounds of (reverse) evolution, involving only four residues. Statistical analysis based on Chebyshev's theorem indicates that this range represents, with $>75\%$ confidence, the total range accessible through mutations at these positions. Second, the wild-type redox potential was not found to be at the middle of the chemically accessible range of reduction potentials [7,8]. Instead, *wt* b_{562} exhibits a redox potential ($\varepsilon^0 = 167$ mV) at the extreme of the chemically accessible range (Fig. 1). More generally, artificial mutations on a variety of electron transport proteins of various folds and modes of chemical ligation induce redox potential changes that span ranges between 100–200 mV (Fig. 1), typically around 150 mV [9–11]. Moreover, it is possible to sample the majority of the chemically accessible range through a small number of mutations in the

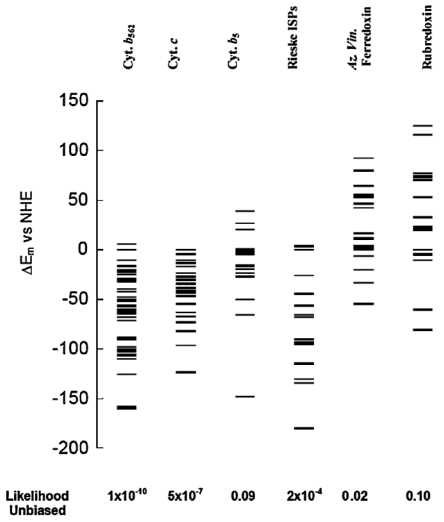

FIG. 1. The shift in redox potential from the wild-type value ($\varepsilon_{\mathrm{WT}} = 0$) for active site mutants of several different cytochromes and iron-sulfur cluster proteins. Maximum likelihood estimation was employed to quantify the extent to which the proteins have evolved toward a redox potential extremum [12]. The likelihood that the true redox potential distribution is unbiased is listed below each protein.

vicinity of the active site, with only minimal concomitant changes to the structure of the scaffold [8].

Most importantly, in nearly every case, these artificial mutations push the redox potential in one direction from the wild-type value (Fig. 1), indicating that this value represents an extremum. In proteins where a few mutations push the potential in the opposite direction (e.g., *Azotobacter vinelandii* Ferredoxin and Rubredoxin) it is nonetheless clear that mutation-induced potential changes are strongly biased statistically in one direction from the wild-type potential. Maximum likelihood estimation (MLE) of the underlying redox potential distributions (see [12]) quantifies this conjecture. For instance, in the case of cytochrome b_{562}, the likelihood that the distribution of redox potentials is unbiased is less than $10^{-8}\%$ (Fig. 1).

This striking observation begs an evolutionary explanation. There is no obvious evolutionary advantage to the redox potentials being extremized by natural selection, since maximal fitness (ATP production) follows from maximization of the proton concentration gradient, which does not bear a simple physical relationship to the redox potentials. Direct evolutionary selection for extremized redox potentials is implausible statistically as well as biophysically, based on additional data regarding the distribution of potentials within the cytochrome c′ family, whose members may be perceived as points along a single dynamical evolutionary trajectory. Two out of four members (cytochrome c′ *Chromatium vinosum* and cytochrome c′ *Rhodospirillum rubrum*) have redox potentials at the lower extreme (-5 and -8 mV, respectively) and two members (cytochrome c′ *Alcaligenes denitrificans* and cytochrome c′ *Rhodopseudomonas palustris*) have potentials $+100$ mV and $+130$ mV [9]. Hence, it appears that the redox potentials of naturally occurring cytochromes are not only extremized, but may be alternately maximized and minimized during the course of evolution through a process that requires relatively few mutations. Even if evolutionary selection did act directly on the redox potentials, it would be necessary to assume the selection pressure oscillates due to environmental dynamics that have no relation to the known function of the ETC. Such a model is not robust to functional form misspecification of the fitness measure, and must be rejected if a simpler fitness measure requiring fewer extrinsic parameters can explain the extremization.

Optimal control theory provides an explanation for the observed behavior that is fully consistent with current evolutionary theory, based on minimal additional assumptions. The terminal oxidation stage of the electron transport chain consists of a linked set of protein-catalyzed substrate oxidation steps, several of which are coupled to protein-catalyzed proton pump steps. Electron transfer to the redox centers alters the pK_a of amino acids involved in proton transport and hence indirectly impacts the efficiency of the proton pumps [12]. The ith enzyme acts on its substrate through a redox process specified by the potential $\varepsilon_i(t)$ as a function of evolutionary time t. The role of this ith enzyme in the fitness measure can be characterized by its current evolutionary state x_i (i.e., the proton gradient produced by its associated proton pump) prescribing the functional utility of the enzyme for the energy transduction process. Since the efficiency of the proton pumps is a function of the redox potentials, it is natural to view the network as an input-output control system, with the controls consisting of $\vec{\varepsilon}(t) = (\varepsilon_1(t), \varepsilon_2(t), \cdots, \varepsilon_N(t))$ and the output being the system state vector $\mathbf{x}(t) = (x_1(t), x_2(t), \cdots, x_N(t))$. Evolution is assumed to be maximizing a biologically beneficial function $\Phi(\mathbf{x})$ of the chain's state (i.e., the total amount of ATP produced) both directly with respect to the state $\mathbf{x}$ as well as indirectly through the controls $\vec{\varepsilon}(t)$.

This evolution of the chain can be modeled in terms of the coevolutionary dynamics [13] of coupled quasispecies sequence families A and B, corresponding to each protein's state and control sequences, respectively. These families are described by the multinomial probability distributions

$$P_A = \{a_k \mid 1 \le k \le n = \kappa^\nu\}$$
$$P_B = \{b_k \mid 1 \le k \le m = \kappa^\mu\},$$

where κ is the monomer alphabet length and ν, μ are the respective sequence lengths. Associated with each state sequence A_k is the value $F_k \in \mathbb{R}$ of a component of the associated physical state vector $\mathbf{x}$ of the protein network (respectively H_k for the control vector $\vec{\varepsilon}$). The expected values of the components of the state and control vectors of the protein network are then $x_i \equiv \langle x_i \rangle = \sum_{k=1}^{n} F_k^{(i)} a_k^{(i)}$, $\varepsilon_i \equiv \langle \varepsilon_i \rangle = \sum_{k=1}^{m} H_k^{(i)} b_k^{(i)}$. The tertiary structure of the protein microenvironment surrounding the redox center

[12] constrains $\varepsilon_i(t)$ to a finite range

$$\varepsilon_i^l(t) \le \varepsilon_i(t) \le \varepsilon_i^u(t). \quad (1)$$

Because protein tertiary structure is less flexible than secondary structure, it is reasonable to assume the bounds $\varepsilon_i^l(t)$ and $\varepsilon_i^u(t)$ vary at a slower rate than the redox potential $\varepsilon_i(t)$ during evolution.

According to the quasispecies model [1], the evolution of the multinomial distribution P_A is given by

$$\dot{a}_k = \sum_{l=1}^{n} W_{kl} R_l(P_B) a_l - D_k(P_B) a_k,$$

where W_{kl} is the probability of producing sequence A_l as an error copy from sequence A_k, R_l is the rate parameter for autocatalytic replication, and D_k is the rate constant for decay of sequence A_k. The effect of the control sequence B on the evolutionary dynamics of the state sequence is represented by the functional dependencies on P_B of the rate constants $R_l(P_B)$, $D_k(P_B)$, which to first-order, can be written $R_l(P_B) = R_l^0 + \sum_{r=1}^{m} R'_{lr} b_r$. In the realistic case that P_A and P_B are sharply peaked with small variance around a master sequence, $\langle \varepsilon_i \rangle \approx H_{\max} b_{\max}$, and we may write $R_l(P_B) = R_l^0 + R'_l b_{\max}$. The rate parameters R_l^0 and D_k^0 are determined by the function $\Phi(\mathbf{x})$ in the fitness measure. It is then straightforward to show that the evolution of the expectation value of each component of the state vector can be written $\frac{dx_i(t)}{dt} = f_i(x_i(t), W_{kl}, F_k, R_l^0, D_k^0, t) + g_i(x_i(t), W_{kl}, F_k, R'_l, D'_k, H_{\max}, t)\varepsilon_i(t)$. If interactions are permitted between state vector components $x_i(t)$, this can be written compactly as

$$\frac{dx_i(t)}{dt} = f_i(\mathbf{x}(t), t) + g_i(\mathbf{x}(t), t)\varepsilon_i(t). \quad (2)$$

A coupled differential equation may be written for $\frac{d\varepsilon_i(t)}{dt}$, which is a function of the same parameters, since the replication of sequence B is contingent on that of A due to their physical linkage within the same protein.

We note that the above evolutionary dynamics framework is based solely on the quasispecies theory and the known function of the ETC. We now show that the observed extremization implies that the rate parameters R'_{lr} and D'_{ks} have been set such that the $\vec{\varepsilon}(t)$'s are optimal for maximizing the increase in evolutionary fitness in a given evolutionary time step dt. This entails a maximization of $\Phi(\mathbf{x})$ with respect to the controls $\vec{\varepsilon}(t)$, subject to the inequality constraint in Eq. (1) and the dynamical constraint in Eq. (2). It is convenient to rewrite the inequality constraint in the form of an equality through the introduction of so-called slack variables $\xi_i(t)$ where

$$G_i(t) \equiv G_i(\varepsilon_i, \varepsilon_i^l, \varepsilon_i^u, \xi_i) \quad (3)$$

$$= (\varepsilon_i(t) - \varepsilon_i^l(t))(\varepsilon_i^u(t) - \varepsilon_i(t)) - \xi_i^2(t) = 0. \quad (4)$$

When each of these slack variables $\xi_i(t)$ is allowed to take on arbitrary real values, then the equality constraint in Eq. (3) is consistent with Eq. (1). We may now define the fitness measure J as having the following form:

$$J = \Phi(\mathbf{x}) + \sum_i \int_0^T \beta_i(t) G_i(t) + \sum_i \int_0^T \lambda_i(t) \left[\frac{d}{dt} x_i - f_i - g_i \varepsilon_i(t) \right] dt. \quad (5)$$

The introduction of the Lagrange multiplier functions $\lambda_i(t)$ and $\beta_i(t)$ will assure that Eqs. (2) and (3) are satisfied, respectively. Equation (5) leads to the biological evolutionary process expressed as $\max_{\vec{\varepsilon}(t)} J$. Maximization of J can be treated as a problem in the calculus of variations, with the unknown functions being the elements of the vectors $\vec{\varepsilon}$, $\vec{\beta}$, $\vec{\xi}$, $\mathbf{x}$, $\vec{\lambda}$. A variation of J with respect to these functions will produce a set of nonlinear equations whose solution would specify the state of the evolving protein network from its initial condition at $t = 0$ to the current time T. Since we have not completely specified the functions $f_i(\mathbf{x}(t), t)$ and $g_i(\mathbf{x}(t), t)$ in Eq. (2), a detailed study of the evolutionary dynamics cannot be carried out here. However, for our purpose of analyzing the mutation data above, we do not need this level of detail. It is sufficient to only consider variations of J with respect to $\vec{\xi}$, $\vec{\beta}$, and $\vec{\varepsilon}$, which produce the following equations:

$$\frac{\delta J}{\delta \xi_i(t)} = -2\beta_i(t)\xi_i(t) = 0, \quad (6)$$

$$\frac{\delta J}{\delta \beta_i(t)} = G_i(t) = 0, \quad (7)$$

$$\frac{\delta J}{\delta \varepsilon_i(t)} = \beta_i(t)[-2\varepsilon_i(t) + \varepsilon_i^l(t) + \varepsilon_i^u(t)] + \lambda_i(t) g_i(t) = 0. \quad (8)$$

We may now analyze the evolutionary consequences of these equations. First, Eq. (6) implies that either $\xi_i(t) = 0$ or $\beta_i(t) = 0$. Considering the first case, $\xi_i(t) = 0$, it is evident from Eqs. (3) and (7) that the redox potential $\varepsilon_i(t)$ must take on the value $\varepsilon_i(t) = \varepsilon_i^u(t)$ or $\varepsilon_i(t) = \varepsilon_i^l(t)$. We may then solve for $\beta_i(t)$ from Eq. (8) by first defining d_i as

$$d_i = -2\varepsilon_i(t) + \varepsilon_i^l(t) + \varepsilon_i^u(t) = \begin{cases} \varepsilon_i^u(t) - \varepsilon_i^l(t), & \varepsilon_i(t) = \varepsilon_i^l(t), \\ \varepsilon_i^l(t) - \varepsilon_i^u(t), & \varepsilon_i(t) = \varepsilon_i^u(t), \end{cases} \quad (9)$$

such that

$$\beta_i(t) = -\lambda_i(t) g_i(t) / d_i(t). \quad (10)$$

The second circumstance, $\beta_i(t) = 0$, implies that $\xi_i(t)$ is free to take on any value prescribed by Eq. (3), given that $\varepsilon_i(t)$ is restricted to the domain specified in Eq. (1). In this case, it is also evident from Eq. (8) that $\lambda_i(t) g_i(t) = 0$, which is expected to only be valid at discrete times $t = t_n$, $n = 1, 2, \cdots$. These time points t_n denote the locations where the control field "bangs" from one extreme limit of the range to the other in Eq. (1) during evolution.

This behavior may be explicitly seen by considering the curvature

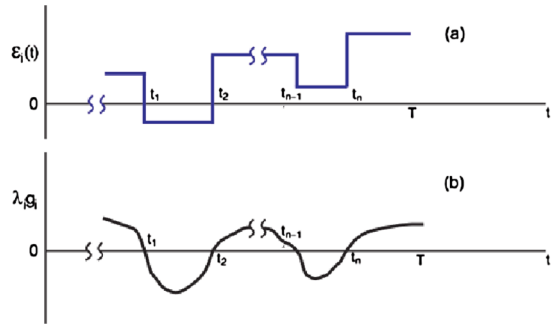

FIG. 2 (color online). (a) The evolution of the redox potential $\varepsilon_i(t)$ for the ith enzyme within optimal control theory. The early evolutionary period near $t \approx 0$ is unspecified. During evolution, the potential "bangs" from its lower and upper accessible values, $\varepsilon_i^l(t)$ and $\varepsilon_i^u(t)$, respectively, at critical times $t_1, t_2, \cdots$ where effective mutations have occurred. The current evolutionary time is T. (b) The evolutionary time dependence of the product $\lambda_i g_i$ of the Lagrange function λ_i and the control coupling function g_i. The zero crossings of $\lambda_i g_i$ occurs at $t_1, t_2, \cdots$ where the redox potential $\varepsilon_i(t)$ undergoes evolutionary jumps in (a).

$$\frac{\delta^2 J}{\delta\xi_i(t)\delta\xi_i(t')} = -2\beta_i(t)\delta(t-t') < 0, \qquad (11)$$

where $\delta(t-t')$ is a Dirac delta function, and the inequality corresponds to requiring that J be maximized. Thus, for the case $\varepsilon_i(t) = \varepsilon_i^u(t)$ in Eq. (9), it follows that $d_i < 0$, thereby corresponding to $\lambda_i(t)g_i(t) > 0$, to assure that Eq. (11) is satisfied. Similarly, in the opposite case of $\varepsilon_i(t) = \varepsilon_i^l(t)$, we have that $d_i > 0$ and that $\lambda_i(t)g_i(t) < 0$. The points t_n, $n = 1, 2, \cdots$ correspond to the times at which $\lambda_i(t)g_i(t)$ changes sign by passing through zero. This behavior is indicated in Fig. 2. The possible evolution of the extremum values $\varepsilon_i^l(t)$ and $\varepsilon_i^u(t)$ is also indicated in the figure.

Importantly, the redox potential data above [7–11] are fully consistent with this analysis of bang-bang control behavior. That is, at the present evolutionary time T, each redox potential $\varepsilon_i(T)$ should be at a locally accessible extreme value. The introduction of artificial mutations in the laboratory could then only take $\varepsilon_i(T)$ away from its extreme value in a consistent direction for each protein, as found above. Moreover, assuming members of the cytochrome c′ family lie along the same evolutionary trajectory, their alternatively maximized and minimized redox potentials are consistent with the above model for $t < T$. We emphasize that this finding of optimality is based solely on statistical inference and variational calculus and does not imply anything about the mechanism by which optimality is achieved. However, the required tuning of the rate constants R_{lr}^l, D_{ks}^l to optimal constant values is straightforward to achieve via reorganization of the protein's tertiary structure [12] through genetic recombination, and avoids the biophysically implausible assumption of direct evolutionary selection for redox potential extremization on an oscillating fitness landscape.

It is important to consider the consequences of J in Eq. (5) containing other costs on the redox potential controls, such that $J \to J - C$. A biologically plausible scenario corresponds to

$$C = \omega \sum_i \int_0^T \left(\frac{d\varepsilon_i(t)}{dt}\right)^2 dt.$$

This places a cost on the rate at which control changes occur due to the quasispecies error threshold, which limits the number of mutations that can be borne by an evolving population per generation [14]. In this case, bang-bang control can still be produced, but with a rounding-off of the sharp corners at the jump times [12].

A natural question concerns the generality of optimal control phenomena in evolutionary dynamics. Optimal control could in principle be operational in any system where evolution of the central function of a protein network is coupled to the evolution of an ancillary protein function. Our results indicate that it is worthwhile to investigate whether the evolutionary dynamics of other biochemical networks with coupled functions exhibit the characteristic signatures of being under optimal control. Bang-bang extremization, while not the only such signature, is simple to detect and provides compelling evidence for underlying OC phenomena. Such optimal control strategies have a particularly natural interpretation within the general framework of evolutionary optimization.

*rajchak@princeton.edu

[1] M. Eigen, J. McCaskill, and P. Schuster, Adv. Chem. Phys. **75**, 149 (1989).
[2] Y. Xia and M. Levitt, Proc. Natl. Acad. Sci. U.S.A. **99**, 10 382 (2002).
[3] R. Chakrabarti, A. M. Klibanov, and R. A. Friesner, Proc. Natl. Acad. Sci. U.S.A. **102**, 12 035 (2005).
[4] S. A. Kauffman, in *Lectures in the Sciences of Complexity*, edited by D. Stein (Addison-Wesley, New York, 1989), pp. 527–618.
[5] A. E. Bryson and Y.-C. Ho, *Applied Optimal Control: Optimization, Estimation and Control* (Hemisphere Publishing, Washington, 1975).
[6] Y. Anraku, Annu. Rev. Biochem. **57**, 101 (1988).
[7] S. L. Springs, S. E. Bass, and G. McLendon, Biochemistry **39**, 6075 (2000).
[8] S. L. Springs, S. E. Bass., G. Bowman, I. Nodelman, C. E. Schutt, and G. McLendon, Biochemistry **41**, 4321 (2002).
[9] A. G. Mauk and G. R. Moore, J. Biol. Inorg. Chem. **2**, 119 (1997).
[10] Z. Xiao, J. Biol. Inorg. Chem. **5**, 75 (2000).
[11] K. Chen, J. Biol. Chem. **274**, 36 479 (1999).
[12] See EPAPS Document No. E-PRLTAO-101-029827 for further details on MLE statistics and background information on the ETC. For more information on EPAPS, see http://www.aip.org/pubservs/epaps.html.
[13] C. Kamp and S. Bornholdt, Phys. Rev. Lett. **88**, 068104 (2002).
[14] S. Bonhoeffer and P. Stadler, J. Theor. Biol. **164**, 359 (1993).